5388 *Macromolecules* **2009**, *42*, 5388–5394
DOI: 10.1021/ma9004633

Macromolecules
ARTICLE

Stretching Semiflexible Filaments and Their Networks

J. R. Blundell* and E. M. Terentjev

Cavendish Laboratory, University of Cambridge, Cambridge CB3 0HE, United Kingdom

Received March 3, 2009; Revised Manuscript Received May 11, 2009

ABSTRACT: Arguments are put forward that mean inextensibility is a valid approximation for semiflexible filaments. Using mean inextensibility, a simple analytical expression for the free energy for single filaments as a function of their end-to-end separation is obtained. This expression contains a term that explicitly represents the internal energy of the filament as well as nonzero temperature effects. Using this free energy, the force−extension relationships of semiflexible filaments and the corresponding nonlinear elasticity of their networks are investigated. Accounting for finite longitudinal compliance of filaments, we identify three distinct scaling regimes in the effective modulus of both single filaments and networks. We find the explicit expressions for crossovers between these scaling regimes; dramatic nonlinear elasticity will only be observed if there is a wide separation between the two crossovers.

1. Introduction

Semiflexible filaments are polymer chains that have a finite rigidity associated with bending of the chain.[1] They occupy a wide middle ground between the freely jointed, flexible chains, which can bend over all length scales, and rigid rods, which cannot bend at all. Flexible filaments are well modeled as Gaussian chains[2] and as such exhibit linear force−extension relations when pulled; they begin to behave nonlinearly only when subject to very large strains.[3] Semiflexible filaments are quite different. They are subject to two competing effects: the thermal motion which promotes bent configurations and the rigidity which promotes straight ones. The interplay between these two effects produces a more complex elastic response, in particular nonlinear elasticity already at small strains.[4−7]

A wide class of biologically relevant filaments are classed as semiflexible including DNA, actin, microtubules, and intermediate filaments. The whole spectrum of carbon nanotubes also falls into this category.[8,9] Comparable in dimensions and bending rigidity are the aggregated protein filaments broadly classed as amyloid fibrils.[10,11] Understanding the behavior of all these filaments has therefore become an area of considerable research. From a theoretical perspective many of the properties such as force−extension relations,[5,7,12,15] distribution functions,[16−19] and buckling[20−22] have been considered before. However, because of mathematical difficulties associated with implementing the chain inextensibility (see below), many of these expressions apply only for very stiff filaments, or conversely for very flexible ones, even though the original papers often claim a broader range of applicability.

In this work we find the compact analytical form for the free energy of a filament as a function of its end-to-end separation using a mean-field method that circumvents the mathematical difficulties of inextensibility in a similar way to some earlier works.[12,23,24] We find that this simple expression for the free energy is valid across the full range of bending stiffness and temperature due to a contribution from the internal potential energy of filament bending as well as nonzero temperature (entropic) effects. This internal energy term is lacking in all expressions for the free energy we know of in the literature.

The paper is laid out in the following way. In section 2 we review the basic theory behind the study of semiflexible filaments. In section 3 we discuss the concept of mean inextensibility and assess how good an approximation it is. Section 4 shows how the free energy of a filament under mean inextensibility can be captured by a very simple free energy function containing just two terms. In section 5 we extend the analysis to include the possibility that filaments can stretch mechanically, increasing their contour length. We then propose that the effects of this model can be seen not only in stretching individual semiflexible filaments but also by applying an external stress to their networks. In section 6 we explore these features by comparing to some experimental data on in vitro actin filaments.

2. Semiflexible Filaments

One of the simplest models that introduces the concept of rigidity to polymer chains is the wormlike chain model (WLC) first proposed by Kratky and Porod.[1] In this model filament rigidity is introduced by associating an energy penalty with filament curvature. The filament is treated as a space-curve $\mathbf{r}(s)$, where s parametrizes the arc length along the curve. The Hamiltonian is built by associating an energy per unit length that scales like the local squared curvature multiplied by A, the bending modulus for the filament:

$$H[\mathbf{r}(s)] = \int_0^L \mathrm{d}s\, \frac{A}{2}\left(\frac{\mathrm{d}^2\mathbf{r}}{\mathrm{d}s^2}\right)^2 \tag{1}$$

For filaments to bend with typical curvatures that are of the same order as their length L requires an energy of the order A/L. For a large class of synthetic and biological filaments, this energy scale is of order k_BT, and therefore thermal fluctuations continuously cause the filament to bend weakly. Such filaments are termed semiflexible as they occupy a middle ground between the Gaussian chains (with no or very weak bending energy) and rigid elastic rods whose characteristic bending energy A/L far exceeds k_BT.

By choosing the contour length to parametrize the curve in the WLC model, we immediately introduce the geometric constraint that $\mathrm{d}\mathbf{r}^2 = \mathrm{d}s^2$, and so by choosing this specific parametrization of the filament, we impose the constraint $(\mathrm{d}\mathbf{r}/\mathrm{d}s)^2 = 1$, for all s[3]. Physically this constraint is a requirement that the filament is locally inextensible (see Figure 1).

*To whom correspondence should be addressed.

 Published on Web 05/29/2009

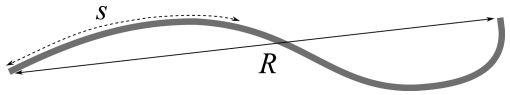

Figure 1. A cartoon semiflexible filament showing the key notations. In the remainder of the paper the separation of a filament is the dimensionless measure of span separation $\mathbf{x} = \mathbf{R}/L$, where $L = \max[s]$ is the full contour length.

In the study of individual filaments as well as their networks it is useful to know the free energy of a single filament as a function of its end-to-end separation **R**. Adopting the reduced measure for end-to-end separation $\mathbf{x} = \mathbf{R}/L$, we will be interested in the free energy $F(\mathbf{x})$. This can be obtained from the constrained partition function in the usual way $F(\mathbf{x}) = -k_B T \ln P(\mathbf{x})$, where $P(\mathbf{x})$ is the (non-normalized) probability that the ends of the filament are separated by a span vector **x**. The probability distribution can be calculated by counting all possible conformations of a filament that have their ends separated by **x** and adding up the probabilities associated with each conformation. This basic partition function can be written in the form of a functional integral over the $\mathbf{r}(s)$ that are constrained to have a separation of **x** and be locally inextensible

$$P(\mathbf{x}) \propto \int \mathcal{D}\mathbf{r} \exp(-H[\mathbf{r}]/k_B T) \tag{2}$$

subject to the explicit constraints:

$$\frac{1}{L}\int_0^L \mathrm{d}s \left(\frac{\mathrm{d}\mathbf{r}}{\mathrm{d}s}\right) = \mathbf{x} \quad \text{and} \quad \left(\frac{\mathrm{d}\mathbf{r}}{\mathrm{d}s}\right)^2 = 1 \tag{3}$$

The integral in (2) subject to the constraints of (3) presents a formidable mathematical problem corresponding to a nonlinear sigma model.[19] Its solution can only be obtained in the form of an infinite series which converges in the limit of flexible chains[16,17] or in the very stiff chain limit.[18,19] The difficulties of evaluating (2) stem from the requirement that the tangent vectors are of unit magnitude. In the following section we explore a method that circumvents these mathematical problems while still retaining the essential physical properties of stiffness and inextensibility.

3. Mean Inextensibility

The essence of the mean-field approach to inextensibility can be seen by writing the δ-function constraint of unit tangent vectors (3) in terms of its Fourier decomposition:[23]

$$\delta\left[\left(\frac{\mathrm{d}\mathbf{r}}{\mathrm{d}s}\right)^2 - 1\right] = \int \mathrm{d}\phi(s) \exp i\phi(s)\left[\left(\frac{\mathrm{d}\mathbf{r}}{\mathrm{d}s}\right)^2 - 1\right] \tag{4}$$

The idea is then to replace the auxiliary field $\phi(s)$ with a constant value of ϕ independent of s. Physically this amounts to relaxing the constraint of rigid local inextensibility to the one of "global inextensibility" that counts contributions to the functional integral (2) whose *average* tangent vectors are of unit length; $\langle(\mathrm{d}\mathbf{r}/\mathrm{d}s)^2\rangle = 1$.

This procedure is analogous to a transformation from the microcanonical ensemble to the canonical ensemble in statistical mechanics and is in essence a mean-field theory. As in the case of all such theories, it is important to consider how valid the approximation is by considering fluctuations about the mean. In the case of statistical mechanics, the particular ensemble one chooses to work in is largely irrelevant as the fluctuations in macroscopic quantities such as the energy scale like $1/\sqrt{N}$, where N is the number of particles in the system and is macroscopically large. In the case of the semiflexible filament we must examine the fluctuations in the length of the tangent vectors away from the locally inextensible value of unity. We calculate these fluctuations using a simple counting argument.

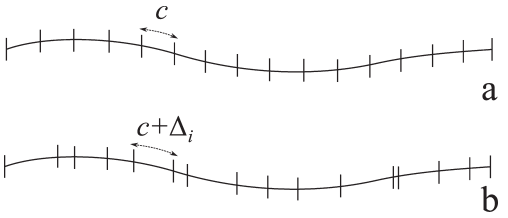

Figure 2. A cartoon illustrating the differences between local inextensibility (a) where the parametrization of the chain is the true arc length and mean inextensibility (b) where the parametrization averages to the true arc length.

Imagine we parametrize the filament not with the continuous arc-length variable s, but with a discrete set of markers placed at interval lengths of $c = L/N$ along the filament (Figure 2a). The continuous parametrization can always be recovered by setting $N \to \infty$. In this picture the local inextensibility constraint (3) is that the contour length between neighboring markers is constant along the entire chain, each marker being separated by c.

The mean-field procedure described above corresponds to the allowing distance between neighboring markers to fluctuate away from c while keeping the number of markers N fixed (this ensures that the *average* distance between neighboring markers remains c). Such a scenario is shown in Figure 2b. We label the arc length between the ith and $(i-1)$th marker $c + \Delta_i$, where Δ_i represents how far the arc length has fluctuated away from the locally inextensible value of c.

Each such arrangement of the N markers along the chain will in general occur with a different probability. This is because the likelihood of a particular configuration occurring is determined by the curvature assigned to that configuration. As the curvature will depend on the placement of the markers, so will the likelihood of seeing that configuration. However, provided the fluctuations Δ_i are small in comparison to the curvature of the filament (to be self-consistently checked), this effect will be small, and so we assume all configurations of markers along the chain occur with equal probability.

We can now calculate the mean-square fluctuation in local arc length by averaging Δ_i^2 over all possible marker configurations using the iterative procedure. For the case of N markers this is

$$\langle\Delta^2\rangle = \frac{1}{\boldsymbol{N}}\prod_{i=1}^{N}\int_{c-\Delta_{i-1}}^{(N-i)c} \mathrm{d}\Delta_i \left[\frac{1}{N}\sum_j (\Delta_j - c)^2\right] \tag{5}$$

where $\boldsymbol{N}$ is the normalizing constant

$$\boldsymbol{N} = \prod_{i=1}^{N}\int_{c-\Delta_{i-1}}^{(N-i)c} \mathrm{d}\Delta_i \tag{6}$$

The limits on this integral arise from considering that the placement of the first marker at $c + \Delta_1$ can be chosen anywhere from 0 to L. The placement of the second can be anywhere in front of the first marker, and so on.

From this expression one finds that the resulting fractional fluctuations in the separations of the markers $(\langle\Delta^2\rangle)^{1/2}/c = [(N-1)/(N+1)]^{1/2}$, which in the limit of a continuously parametrized filament ($N \to \infty$) approaches unity. The fluctuations are therefore well-bounded, which is to say that the major contributions to the functional integral come from filaments whose tangent vectors are close to unity. We now continue, aiming to obtain the free energy of a filament having invoked the mean-field inextensibility approximation.

4. Filament Free Energy

Using this mean-field approximation, the expression for the probability distribution reduces to

$$P(\mathbf{x};L) \propto \int \mathscr{D}\mathbf{r}\, e^{-H[\mathbf{r}]/k_BT}\delta[\langle(d\mathbf{r}/ds)^2\rangle - 1] \tag{7}$$

subject to the boundary conditions $(\mathbf{r}(L) - \mathbf{r}(0))/L = \mathbf{x}$. This functional integral can now be performed with no further approximations, and the result can be written as an integral over the auxiliary field ϕ (see ref 27 for details). Moreover, the probability distribution turns out to depend on its variables only through a single nondimensional combination of parameters

$$\gamma = \frac{A}{2k_BTL}(1-x^2)$$

For a chain in d dimensions the general result is

$$P(\gamma) = \int d\phi\, e^{i\gamma\phi}\left(\frac{\sqrt{i\phi}}{\sin\sqrt{i\phi}}\right)^{d/2} \tag{8}$$

This exact expression (for the non-normalized probability) uses only the approximation of mean inextensibility and is valid for all values of bending stiffness. In two dimensions the integral can be solved exactly via contour integration[27] and closely agrees with previous expressions obtained in the literature.[18] In the relevant case of $d = 3$ the integral cannot be performed analytically but is easily evaluated numerically due to its dependence only on a single parameter γ.

In the past, several approximate analytical expressions have been offered to represent the probability $P(\mathbf{x})$ in 3 dimensions, some used quite widely.[7,12,19,24] There is however a flaw in many of these proposed distribution functions. If one calculates free energy of a filament using the formula $F = -k_BT \ln P$, none of these previously proposed distribution functions possess a term that represents the internal energy of a bent filament. Physically, one should expect such a term, which would survive in the limit $T \to 0$. Such an internal energy term is lacking in these approximate distributions and therefore so must be some essential physics. To this end, we propose the simplest functional dependence of $P(\gamma)$ which captures the correct physical behavior both in the zero temperature and high temperature limits. We find that the simple interpolation for the partition function

$$P(\gamma) = \exp\left[-\pi^2\gamma - \frac{1}{\pi\gamma}\right] \tag{9}$$

is the analytical form that possesses both an internal energy term and an entropic term in the resulting free energy. This remarkably simple form is a very good approximation to the numerical integral (8) for $d = 3$. It captures all essential features of the curve, scaling in the correct way for large and small values of γ. A comparison of the interpolation formula (9) with the numerically evaluated values of the integral (8) in 3-d is shown in Figure 3. For comparison, this figure also plots the famous and widely used formulas due to Marko and Siggia[7] and Ha and Thirumalai.[12] All these and other analytical expressions agree in the limit $\gamma \to 0$, which corresponds to the very long, highly stretched, or flexible chains eventually reaching the Gaussian limit. There are, however, spectacular disagreements in the limit of stiff or short chains (at $\gamma \geq 1$), where the limit of pure bending energy is not present in earlier formulations.

Substituting the expression for γ, we find that within the mean inextensibility approximation there is a simple expression for the free energy of a single chain as a function of extension, given by

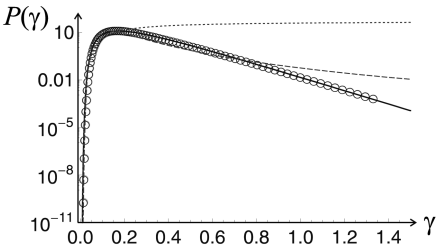

Figure 3. Comparison of numerical values for the 3-d integral in (8) (circles) with the interpolation formula (9), plotted as a solid line. The interpolation fits very well, which is emphasized by the logarithmic P-axis, in particular, capturing the correct scaling at large and small γ with the maximum at the correct value. For comparison, the dashed line shows the Ha−Thirumalai expression[12] and the dotted line the Marko−Siggia expression.[7]

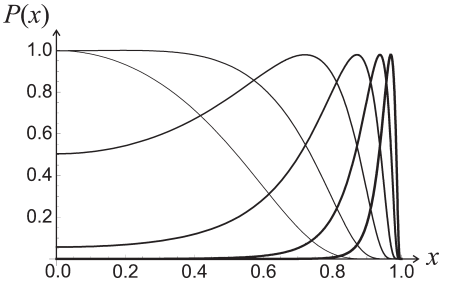

Figure 4. Non-normalized probability distribution plots $P(x)$ for filaments of increasing stiffness (in order of increasing line width): $A/k_BTL = 0.125$, 0.25, 0.5, 1.0, 2.0, and 4.0.

$$F(x) = \frac{A\pi^2}{2L}(1-x^2) + \frac{2(k_BT)^2L}{\pi A(1-x^2)} \tag{10}$$

This form of the chain free energy differs from previous results obtained in the literature[7,12,19] in that it clearly delineates the roles of bending energy and the nonzero temperature (entropic) effects in the free energy. If one takes the limit of a very short filament, or equivalently a filament with a very large bending modulus A, then the potential energy term dominates over the entropic term, and the free energy of the filament is simply the bending energy of an elastic rod. In this limit the formula reassuringly recovers the bending energy of a macroscopic rod that is derived in the small bending regime using a variational principle: $U \approx (A\pi^2/L)(1 - x)$.[26,29]

In the opposite limit of small bending modulus or a very long filament, the entropic term dominates the free energy. In this regime the minimum of the free energy is at zero extension, and expanding about this minimum, in the leading order one recovers the free energy of a Gaussian chain with step length (or the persistent length) $l_p \sim A/k_BT$ (deviation from this Gaussian behavior will occur at larger extensions because true Gaussian chains are infinitely extensible). We illustrate these limits and the crossover between them by plotting the non-normalized probability distributions for filaments of increasing stiffness in Figure 4.

5. Extensible Filaments

The previous analysis has only accounted for the competing effects of bending energy (which favors a straight filament) and entropic effects (which favor bent conformations). Under tension we might expect a filament to also mechanically stretch along its contour length as well as to stretch entropically (by "pulling out" thermal fluctuations). Such mechanical stretching has been observed in both experiments on individual DNA filaments[13] and in

recent Monte Carlo simulations.[14] How does a finite longitudinal compliance alter properties such as the force−extension relation and stiffness of the filament? The simple form of the free energy−extension relation that results from a mean-field analysis enables this to be calculated.

In general, one can include the effect of finite extensibility on chain statistics by considering the partition sum (2) where the Hamiltonian is modified to include a term representing the energetic penalty associated with inducing a strain field $\varepsilon(s)$ along the filament contour. Such a method has been thoroughly explored in ref 15. Here we offer a simpler approach which nonetheless recovers the essential physics.

In (10) we have an expression for the free energy of a single filament that cannot alter its contour length. Under tension a semiflexible filament will bend only weakly and therefore will have a separation x close to unity. Using this fact, we can approximate $1 - x^2 \approx 2(1 - x)$ provided the chains we are interested in are always under tension (the analysis of buckling under compressive force is given in ref 22). The free energy for such filaments can therefore be well approximated by

$$F(x) = \frac{A\pi^2}{L}(1-x) + \frac{(k_B T)^2 L}{\pi A(1-x)} \tag{11}$$

The force−extension relation for this inextensible filament can then be obtained in the usual manner by taking the derivative of the free energy with respect to the actual span separation $R = xL$:

$$f(x) \approx -f_c + \frac{(k_B T)^2}{\pi A(1-x)^2} \tag{12}$$

Here we have used the shorthand that $A\pi^2/L^2 = f_c$ with f_c the classical Euler buckling force for a pinned filament of bending modulus A and length L.[29] In agreement with previous theoretical[5−7] and experimental[4] results, the force diverges as $(1 - x)^2$, which is a direct consequence of filament inextensibility. In reality, filaments can also deform in response to an applied force by mechanically stretching. The mechanical spring constant k_m associated with longitudinal deformation of the filament material is governed by the Young's modulus of the filament material and its geometry; $k_m = (Y/L)\int dS$ where the integral is over the cross-sectional area of the filament and can be applied to any cross-sectional shape.[25] We assume in this analysis that the Young's modulus of the filament is a constant independent of strain. This is a good approximation for modest strains though will inevitably fail at very large strains where nonlinear effects and eventual filament rupture will occur. Such issues have recently been discussed in the context of overstretched DNA[30] and β-sheet aggregated peptides.[31] Considering two relevant examples: an actin filament of length 10 μm has a mechanical stretch modulus $k_m \approx 5$ pN/nm[32] while a microtubule of the same length has a slightly larger stretch modulus of $k_m \approx 15$ pN/nm.[33]

When subjected to a tension force f, the filament can therefore increase its contour length in response to the applied force f by mechanically stretching to a new length $L_f = L + f/k_m$.[5] Substituting this altered length into the force−extension relation (12) and solving for the extension $x(f)$, we obtain the following relationship for an extensible filament:

$$x(f) = \left(1 + \frac{f}{k_m L}\right)\sqrt{1 - \frac{(k_B T)^2(L + f/k_m)}{\pi A(f + f_c)}} \tag{13}$$

where L is the original, unstretched contour length.

Similar results have been obtained before by Odijk[5] and Lipowsky.[15] A plot of the force−extension relation for an actin filament ($L = 10\,\mu$m) is shown in Figure 5. A key feature of this relationship is that mechanical stretching becomes the softer mode at large forces and results in the filament being able to extend by increasing its contour length, an effect observed experimentally in both DNA[34] and actin.[35]

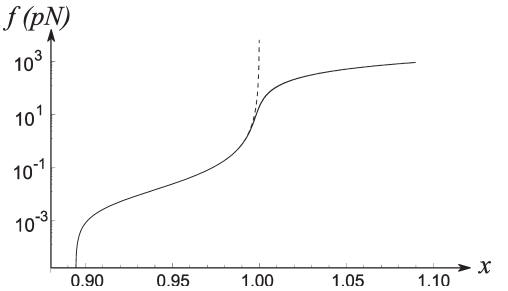

Figure 5. Logarithmic force−extension plot for an inextensible (dashed line) and extensible (solid line) filament. Filament parameters correspond to those of an actin filament $L = 10\,\mu$m, $l_p = 17\,\mu$m, $Y = 2$ GPa, and filament diameter $d = 7$ nm. Deviation of the solid line from the dashed line at high forces is due to mechanical stretching of the filament.

With the simple expression presented here, we can quantify the interesting crossover region from the entropic stretching regime to the mechanical stretching regime by examining the spring constant for a single filament as a function of the applied force.

For an inextensible filament the effective spring constant, which is now purely entropic, is obtained by taking the derivative of the force−extension relation (12):

$$K_e(x) = \frac{2(k_B T)^2}{\pi A L(1-x)^3} \tag{14}$$

This is a measure of the resistance of the fluctuating filament to changes in span separation. As one would expect, this entropic stiffness K_e becomes increasingly large as the filament becomes almost fully extended and diverges at full extension $x \to 1$. Given the explicit functions $K_e(x)$ and $f(x)$, we can eliminate the separation variable x to express the entropic stiffness of a single inextensible filament as a function of the applied force f. The result is

$$K_e(f) = k_e(1 + f/f_c)^{3/2} \tag{15}$$

where

$$k_e = \frac{2\pi^{7/2}A^2}{k_B T L^4} \propto k_B T \frac{l_p^2}{L^4}$$

is the linear response modulus and $l_p = A/k_B T$ is the persistence length of the filament. We observe from this result that what controls the crossover into nonlinear entropic stretching is the classical Euler buckling force $f_c = A\pi^2/L^2$. For forces $f < f_c$ the stiffness remains constant, and the filament is in the linear entropic regime, in a similar manner to classical Gaussian chains. For forces $f < f_c$ the filament begins to behave nonlinearly, with the chain stiffness scaling like $f^{3/2}$. These limits agree with the scaling relations of ref 36 for high and low f; however, here we have presented the full expression that quantitatively describes the crossover from the linear to nonlinear stretching regime as well as the reasons why.

Now we can include the effects of a finite stretching modulus k_m. The filament now has two possible modes of deformation, either mechanical stretch governed by modulus k_m or entropic stretch governed by modulus $K_e(f)$. The filament is therefore

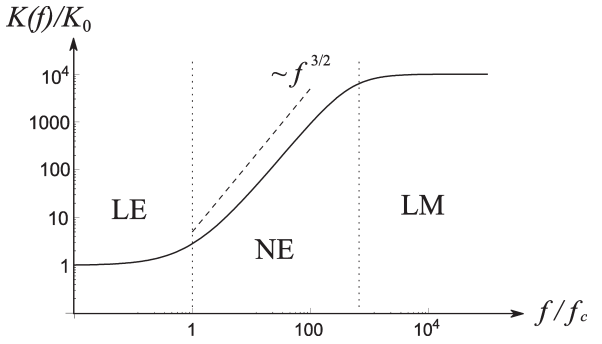

Figure 6. Stiffness as a function of applied force for an extensible semiflexible filament. The regions illustrated are linear entropic (LE) at low forces, nonlinear entropic (NE) at intermediate forces, and linear mechanical (LM) at high forces. A separation of the two crossovers (marked by the two dotted lines) results in there being a clear middle region where the filament is highly nonlinear. This is plotted for a filament with $k_m/k_e = 10^4$.

"composed" of two springs in series, one of spring constant k_m the other $K_e(f)$, with a resulting modulus

$$\frac{1}{K} = \frac{1}{k_m} + \frac{1}{k_e}(1 + f/f_c)^{-3/2} \tag{16}$$

The various scaling regimes of the effective stiffness of filaments at low, medium, and high tensile forces are now apparent. For small tensile forces $f < f_c$ the modulus of the filament is a constant, $K_0 = (k_m^{-1} + k_e^{-1})^{-1}$, and is termed linear entropic (LE). At intermediate forces $f \geq f_c$ the entropic part is scaling like $f^{3/2}$, and this regime is termed nonlinear entropic (NE). At large tensile forces (outlined below) the filament has to stretch mechanically and so behaves linearly once again; this regime is therefore termed linear mechanical (LM). These three regimes are illustrated in Figure 6.

As we have seen above, the crossover LE → NE is dictated by the value of the Euler buckling force $f_c = A\pi^2/L$. Using $A/k_BT = l_p$, we see that the nonlinear entropic stretching begins at forces $\sim k_BTl_p/L^2$. Actin filaments in cells have $L \approx l_p \approx \mu$m, giving a typical crossover force on the order of 10^{-3} pN. For microtubules persistence lengths are on the order of millimeters so that typical crossover forces to the nonlinear stretching regime are on the order of a single pN.

The crossover from nonlinear entropic to mechanical stretching (NE → LM) occurs when $f \sim f_c(k_m/k_e)^{2/3}$. Substituting in the expressions for the linear moduli in terms of the physical parameters for a filament, we see that the crossover to mechanical stretching occurs at forces $f \sim k_BT(l_p/d^4)^{1/3}$. Actin has a diameter of $d \sim 10^{-8}$ m and so will begin to mechanically stretch when subjected to forces $f \sim 0.1$ pN—far larger than the forces at which the LE → NE transition occurs. Microtubules are hollow (they have a smaller effective cross section) which reduces k_m in proportion to k_e, and the crossover to mechanical stretching occurs at forces $f \sim$ pN. This suggests that for very stiff filaments such as microtubules where $l_p \gg L$ the crossover forces between the regions LE → NE and NE → LM converge; that is, for such filaments mechanical stretching is always relevant while the nonlinear force−extension regime NE is hard to identify.

6. Networks of Filaments

We now turn to the mechanical properties of networks composed of semiflexible filaments. Specifically, we would like to explore how the previous analysis of stiffness−force relationships for extensible filaments might impact on the properties of networks. Our approach is intentionally reductionist focusing on the scaling of the network stiffness as a function of applied stress, in a similar manner to ref 36. The exact treatment of

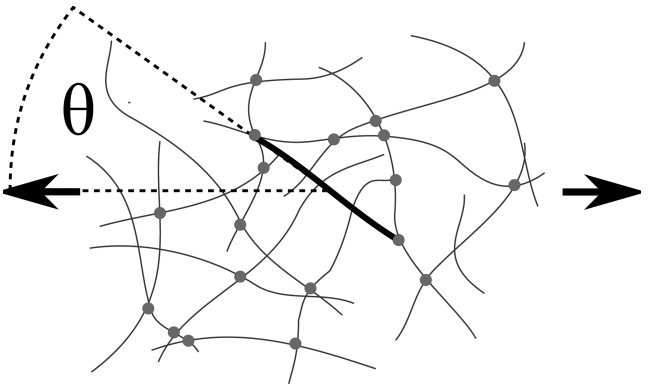

Figure 7. Schematic of an isotropic cross-linked semiflexible network. The direction of the applied strain is shown by the arrows. We highlight in bold one of the strands in the network (a connection between cross-links) that lies at an angle θ to the axis of principal strain.

polymer networks must include careful orientational averaging of strands with respect to the principal axes of applied strain,[37] the possibility that there are nonaffine deformations[38] and anisotropies in the orientations of filaments,[39] and the effect of the stiffness of the cross-links themselves.[41]

We can examine the importance of orientational effects in networks by looking at the deformation of an initially isotropic network to a uniaxial affine strain field $\lambda_{xx} = \lambda$, $\lambda_{yy} = 1/\sqrt{\lambda}$, $\lambda_{zz} = 1/\sqrt{\lambda}$. Any strand of the network linking two cross-links is assumed to be an independent filament (the phantom chain approximation[42]). We consider a filament oriented at an angle θ to the x axis (see Figure 7). The result of this deformation on the filament is a rotation (which does not affect the energy) and a stretch (or compression) that changes the end-to-end separation to a new value:

$$x' = x_0\sqrt{\sin^2\theta/\lambda + \lambda^2\cos^2\theta} \tag{17}$$

where x_0 is the initial end-to-end separation of the filament ends from (12) given by $x_0 = 1 - k_BT/(\pi Af_c)^{1/2}$. Whether a filament is stretched or compressed depends on θ, the angle to the axis of principal strain. The stretch modulus of a single filament increases rapidly upon filament extension (14). This suggests that filaments that are stretched under the deformation contribute the most to the modulus of the network as a whole. To highlight this, we plot the individual contributions of filaments to the modulus of the entire network as a function of the original angle θ the filament makes with respect to the axis of principal strain (Figure 8). The plot corresponds to an isotropic network undergoing affine incompressible uniaxial strain. We do indeed see that the majority of the contribution to the modulus (and the stress) comes from chains oriented around the principal strain axes and that this approximation becomes better at larger and larger strains.

We can quantify the magnitude of the strains over which this approximation holds. Initially, the filament has an equilibrium end-to-end separation of $x_0 = 1 - k_BT/(\pi Af_c)^{1/2} \sim 1 - L/\pi^{3/2}l_p$. Because free energy (and hence the force and stiffness) begin to diverge close to full extension, the filaments that have been strained to full extension will contribute most to the modulus. Filaments oriented with the axis of principal strain will reach this point when the network is strained by approximately

$$\lambda \approx \frac{1}{1 - L/\pi^{3/2}l_p} \tag{18}$$

For networks of stiff filaments $L/l_p < 1$ so Taylor expanding we see that filaments oriented along the principal strain axis

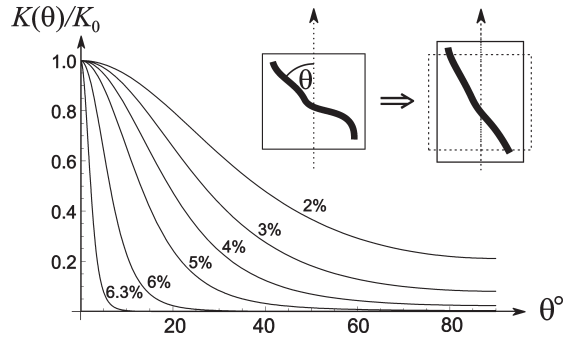

Figure 8. Plots of the modulus of a filament as a function of its initial angle to the axis of principal strain at increasing values of strain. The plot corresponds to an isotropic network of filaments undergoing affine uniaxial strain. Note that at larger strains the majority of the contributions to the modulus come from chains oriented close to the principal strain axis.

dominate the network modulus when $\lambda \approx 1 + L/\pi^{3/2}l_p$. For semiflexible networks these strains are modest—on the order of 1%−5%.

The above conclusion that filaments oriented along the axis of principal strain are the key determinants of stiffness is based on an assumption that the network undergoes affine strain and that it is isotropic. This assumption will not hold for all network geometries. Indeed, for networks that are highly anisotropic,[39] or where the filaments are rigidly constrained to have a fixed angle[40] or are only weakly cross-linked so as to be just above the rigidity transition,[43] the stiffness of the network will be determined by nonaffine deformations at low strains.[38,43] However, even these networks will, at larger strains, enter a regime where the dominant contribution to the modulus must come from stretched filaments as this is the largest energy scale in the system. Networks in which the cross-links themselves have a finite stiffness[41] are amenable to this model as well. In this case the mechanical stretch modulus k_m in the model would be a combination of the mechanical stretch modulus of both the filament (k_f) and cross-links (k_{cl}) in the form $k_m^{-1} = k_f^{-1} + k_{cl}^{-1}$. Physically, this amounts to considering a cross-link and filament as springs in series, where the modulus will largely be determined by the softer of the two spring stiffnesses.

With this is mind we propose that the stiffness of networks can be captured by replacing the idea of an isotropic network with an ensemble of filaments all of which are oriented along the direction of principal strain. Physically, we are saying that only a fraction of filaments contribute to the resulting modulus and that these filaments are essentially oriented along the axis of principal extension.

If the average area occupied by each of these filaments is ξ^2, then when a stress σ is applied to the network, the average tension in the contributing filaments is $f \sim \sigma\xi^2$. The average strain that results from this applied stress will be $\Delta L/L = f/KL = \sigma\xi^2/KL$. The contribution of these filaments to the modulus of the network can then be related to the stiffness of the individual filaments via

$$G = \frac{\partial\sigma}{\partial\lambda} = \frac{L}{\xi^2}K \tag{19}$$

Substituting the expression for K from (16), we can therefore write down the analogous expression that, instead of relating the stiffness of a single filament to the force exerted on that filament, now relates the modulus of a network to the applied stress:

$$G(\sigma) = G_0\left(\frac{k_e}{k_m} + (1 + \sigma/\sigma_c)^{-3/2}\right)^{-1} \tag{20}$$

where direct substitution of the defined quantities yields

$$\sigma_c = \frac{f_c}{\xi^2} \quad G_0 \sim \frac{A^2}{k_B T L^3 \xi^2} \quad \frac{k_e}{k_m} \sim \frac{Ad^2}{k_B T L^3} \tag{21}$$

The expression (20) captures the nonlinear elastic behavior of semiflexible networks for the entire range of applied stresses (until of course the network is irreversibly ruptured). At low stresses $\sigma < \sigma_c$ the modulus is approximately constant with a linear-response value G_0. The origin of this is that we are only exploring the linear entropic stretching regime of the constituent filaments.

At very large stresses $\sigma \geq \sigma_c(k_m/k_e)^{2/3}$ the modulus is again a constant with a value $G \sim k_m L/\xi^2$. Physically, this arises from the mechanical stretching of constituent filaments which are aligned along the principal extension, and hence at large stresses we expect the modulus to be largely independent of temperature.

For intermediate stresses $\sigma_c < \sigma < \sigma_c(k_m/k_e)^{2/3}$ behaves nonlinearly and, provided there is a separation of the two crossovers σ_c and $\sigma_c(k_m/k_e)^{2/3}$, the modulus begins to scale like $\sigma^{3/2}$. The scaling of $G(\sigma)$ at low and intermediate stresses has been derived in a similar framework before;[36] however, here we extend this result to be applicable to extensible filaments. Our analysis is able to quantitatively describe the crossover from linear entropic to nonlinear entropic stretching and the second crossover, from nonlinear entropic to linear mechanical stretching, as in the case for individual filaments.

This analysis enables us to make various predictions about the form of modulus−stress curves that can be measured for in vitro semiflexible networks.[44] The crossover from a linear entropic regime to a nonlinear entropic regime is governed by the critical stress $\sigma_c \sim A/L^2\xi^2$. For isotropic semiflexible networks the average distance between alligned filaments $\xi \sim L$.[45] The length between entanglements in semiflexible networks scales like $L \sim c^{-1/2}$ where c is the concentration of polymer material.[46] The crossover stress therefore scales like $\sigma_c \sim A/L^4 \sim c^2$. We verify this in Figure 9 by plotting experimental values for σ_c (extracted from the data of ref 44 by means of tangent intercepts) as a function of concentration. We do indeed observe an approximately quadratic scaling of the crossover stress σ with concentration.

Furthermore, our analysis suggests that the scaling $G \sim \sigma^{3/2}$ proposed in ref 44 only occurs if there is a wide separation between σ_c (the critical stress at which NL scaling begins) and $\sigma_c(k_m/k_e)^{2/3}$ (the stress at which LM stretching becomes important). If these two stress scales are of the same order, then a much weaker $G(\sigma)$ scaling would be observed.

7. Conclusions

Mean inextensibility is a good approximation that can circumvent some of the mathematical difficulties associated with the wormlike chain model when it is applied to semiflexible polymers or filaments. Although the tangent vectors are no longer regarded of rigidly unit magnitude along the entire chain, the mean inextensibility approximation ensures that the average tangent vector is of unit magnitude and the fluctuations away from this mean are always well-bounded.

Invoking mean inextensibility allows one to obtain a compact expression for the probability distribution of semiflexible filaments that depends on a single combination of physical parameters. An interpolation formula for the free energy of a single filament follows from this, which matches the exact numerical result almost perfectly. There must be an underlying rigorous mathematical reason for this (and similar expressions we can write down for arbitrary dimension d); unfortunately, we cannot see it at the moment. The filament free energy contains two separate terms: one accounts for the internal energy of a bent

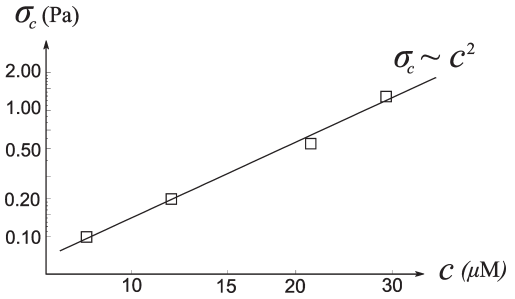

Figure 9. Plot showing the experimental values of σ_c as a function of concentration for the data of ref 44. The scaling of the solid line shows the quadratic dependence of σ_c on concentration.

filament, while the other accounts for nonzero temperature (entropic) effects. This free energy expression captures the correct behavior for the entire range of temperatures and stiffnesses, in particular the limits of a Gaussian chain (for very low stiffness) and the limits of a rigid rod (very large stiffness or low temperature) as well as the crossover between them.

The expression for the filament free energy can be applied to study force−extension relations and stiffness−extension relations in semiflexible filaments and networks. A simple analysis predicts that the crossover into a nonlinear elastic regime is controlled by the classical Euler buckling force for filaments $f_c = A\pi^2/L^2$. This nonlinear elasticity only survives provided we do not cross over into a subsequent mechanical-stretching regime, which is controlled by the force $f_c(k_m/k_e)^{2/3}$. For filaments where these crossovers are very different (as for DNA), a scaling of stiffness with applied force $K \sim f^{3/2}$ would be observed in the middle nonlinear regime. If these crossover values converge to one another (as for microtubules), no such clear scaling would be observed and the mechanical stretching is always relevant.

The effect of finite stretch moduli on stiffness−stress $G(\sigma)$ relationships that we present here should be observable in a wide variety of stiff networks. In particular, any network that contains both entropic filaments and filaments with finite stretch moduli should show the distinct scaling regimes presented in this paper. Candidates that could show such behavior would be fibrin networks found in blood clots[47] and cross-linked actin networks.[44] Semiflexible networks where the cross-links themselves have finite stretch moduli[41] could also be candidates for the work presented here.

References and Notes

(1) Kratky, O.; Porod, G. *Recl. Trav. Chim.* **1949**, *68*, 1106.
(2) Flory, P. J. *Statistical Mechanics of Chain Molecules*; Interscience: New York, 1989.
(3) Yamakawa, H. *Modern Theory of Polymer Solutions*, 1st ed.; Harper Row: New York, 1971.
(4) Smith, S. B.; Finzi, L.; Bustamante, C. *Science* **1992**, *271*, 795.
(5) Odijk, T. *Macromolecules* **1995**, *28*, 4796.
(6) Fixman, M.; Kovac, J. *J. Chem. Phys.* **1973**, *58*, 1564.
(7) Marko, J. F.; Siggia, E. D. *Macromolecules* **1995**, *28*, 8759.
(8) Wong, E. W.; Sheehan, P. E.; Lieber, C. M. *Science* **1997**, *277*, 1971.
(9) Falvo, M. R.; Clary, G. J.; Taylor, R. M.; Chi, V.; Brooks, F. P.; Washburn, S.; Superfine, R. *Nature (London)* **1997**, *389*, 582.
(10) Smith, J. F.; Knowles, T. P. J.; Dobson, C. M.; MacPhee, C. E.; Welland, M. E. *Proc. Natl. Acad. Sci. U.S.A.* **2006**, *103*, 15806.
(11) Sagis, L. M. C.; Veerman, C.; van der Linden, E. *Langmuir* **2004**, *20*, 924.
(12) Ha, B.-Y.; Thirumalai, D. *J. Chem. Phys.* **1997**, *106*, 4243.
(13) Bustamante, C.; Smith, S. B.; Liphardt, J.; Smith, D. *Curr. Opin. Struct. Biol.* **2007**, *93*, 37.
(14) Buehler, M. J.; Wong, S. Y. *Biophys. J.* **2007**, *93*, 37.
(15) Kierfeld, J.; Niamploy, O.; Sa-yakanit, V.; Lipowsky, R. *Eur. Phys. J. E* **2004**, *14*, 17.
(16) Daniels, H. E. *Proc. Roy. Soc. Edinburgh* **1952**, *63A*, 290.
(17) Hermans, J. J.; Ullman, R. *Physica* **1952**, *18*, 951.
(18) Wilhelm, J.; Frey, E. *Phys. Rev. Lett.* **1996**, *77*, 2581.
(19) Hamprecht, B.; Kleinert, H. *Phys. Rev. E* **2005**, *71*, 031803.
(20) Odijk, T. *J. Chem. Phys.* **1998**, *108*, 6923.
(21) Emanuel, M.; Mohrbach, H.; Sayar, M.; Schiessel, H.; Kulic, I. M. *Phys. Rev. E* **2007**, *76*, 061907.
(22) Blundell, J. R.; Terentjev, E. M. *Soft Matter*, submitted.
(23) Gupta, A. M.; Edwards, S. F. *J. Chem. Phys.* **1993**, *98*, 1588.
(24) Winkler, R. G. *J. Chem. Phys.* **2003**, *118*, 2919.
(25) Landau, L. D.; Lifshitz, E. M. *Theory of Elasticity*, 3rd ed.; Butterworth Heinemann: Oxford, 1986.
(26) Frey, E. *Adv. Solid State Phys.* **2001**, *41*, 345.
(27) Blundell, J. R.; Terentjev, E. M. *J. Phys. A: Math. Theor.* **2007**, *40*, 10951.
(28) Kleinert, H.; Chervyakov, A. *J. Phys. A: Math. Theor.* **2006**, *39*, 8231.
(29) Timoshenko, S. *Theory of Elastic Stability*, International Student Edition; McGraw-Hill: Singapore, 1963.
(30) Rouzina, I.; Bloomfield, V. A. *Biophys. J.* **2001**, *80*, 882.
(31) Keten, S.; Buehler, M. J. *Phys. Rev. E.* **2008**, *78*, 061913.
(32) Higuchi, H.; Yanagida, T.; Goldman, Y. E. *Biophys. J.* **1995**, *69*, 1000.
(33) Howard, J. Sinauer Associates, Inc.: Sunderland, MA, 2001.
(34) Cluzel, P.; Lebrun, A.; Lavery, R.; Viovy, J.-L.; Chatenay, D.; Caron, F. *Science* **1996**, *271*, 792.
(35) Liu, X.; Pollack, G. H. *Biophys. J.* **2002**, *83*, 2705.
(36) Mackintosh, F. C.; Kas, J.; Janmey, P. A. *Phys. Rev. Lett.* **1995**, *75*, 4425.
(37) Kutter, S.; Terentjev, E. M. *Eur. Phys. J. E* **2002**, *8*, 539.
(38) Heussinger, C.; Frey, E. *Phys. Rev. Lett.* **2006**, *97*, 105501.
(39) Dalhaimer, P.; Discher, D. E.; Lubensky, T. C. *Nat. Phys.* **2007**, *3*, 354.
(40) Ovijit, C.; Parekh, S. H.; Fletcher, D. A. *Nature (London)* **2007**, *445*, 295.
(41) Broedersz, C. P.; Storm, C.; Mackintosh, F. C. *Phys. Rev. Lett.* **2008**, *101*, 118103.
(42) Deam, R. T.; Edwards, S. F. *Philos. Trans. R. Soc. London, A* **1976**, *280*, 317.
(43) Head, D. A.; Levine, A. J.; Mackintosh, F. C. *Phys. Rev. E* **2003**, *68*, 061907.
(44) Gardel, M. L.; Shin, J. H.; MacKintosh, F. C.; Mahadevan, L.; Matsudaira, P.; Weitz, D. A. *Science* **2004**, *304*, 1301.
(45) Colby, R. H.; Rubenstein, M.; Viovy, J. L. *Macromolecules* **1992**, *25*, 996.
(46) Schmidt, C. F.; Baermann, M.; Isenberg, G.; Sackmann, E. *Macromolecules* **1989**, *22*, 3638.
(47) Weisel, J. W. *Biophys. Chem.* **2004**, *112*, 267.